AJNR

Quantification of Orbital Apex Crowding for Screening of Dysthyroid Optic Neuropathy Using Multidetector CT

A.C.P. Gonçalves, L.N. Silva, E.M.M.S. Gebrim and M.L.R. Monteiro

AJNR Am J Neuroradiol 2012, 33 (8) 1602-1607
doi: https://doi.org/10.3174/ajnr.A3029
http://www.ajnr.org/content/33/8/1602

ORIGINAL RESEARCH

Quantification of Orbital Apex Crowding for Screening of Dysthyroid Optic Neuropathy Using Multidetector CT

A.C.P. Gonçalves
L.N. Silva
E.M.M.S. Gebrim
M.L.R. Monteiro

BACKGROUND AND PURPOSE: DON, a serious complication of GO, is frequently difficult to diagnose clinically in its early stages because of confounding signs and symptoms of congestive orbitopathy. We evaluated the ability of square area measurements of orbital apex crowding, calculated with MDCT, to detect DON.

MATERIALS AND METHODS: Fifty-six patients with GO were studied prospectively with complete neuro-ophthalmologic examination and MDCT scanning. Square measurements were taken from coronal sections 12 mm, 18 mm, and 24 mm from the interzygomatic line. The ratio between the extraocular muscle area and the orbital bone area was used as a CI. Intracranial fat prolapse through the superior orbital fissure was recorded as present or absent. Severity of optic nerve crowding was also subjectively graded on coronal images. Orbits were divided into 2 groups (with or without clinical evidence of DON) and compared.

RESULTS: Ninety-five orbits (36 with and 59 without DON) were studied. The CIs at all 3 levels and the subjective crowding score were significantly greater in orbits with DON ($P < .001$). No significant difference was observed regarding intracranial fat prolapse ($P = .105$). The area under the ROC curves was 0.91, 0.93, and 0.87 for CIs at 12, 18, and 24 mm, respectively. The best performance was at 18 mm, where a cutoff value of 57.5% corresponded to 91.7% sensitivity, 89.8% specificity, and an odds ratio of 97.2 for detecting DON. A significant correlation ($P < .001$) between the CIs and VF defects was observed.

CONCLUSIONS: Orbital CIs based on area measurements were found to predict DON more reliably than subjective grading of orbital crowding or intracranial fat prolapse.

ABBREVIATIONS: CI = crowding index; DON = dysthyroid optic neuropathy; GO = Graves orbitopathy; HU = Hounsfield unit; MDCT = multidetector CT; ROC = receiver operating characteristic; SAP = standard automated perimetry; VA = visual acuity; VF = visual field; WL = window level; WW = window width

GO is an autoimmune inflammatory process affecting the orbital and periorbital tissues, mainly the extraocular muscles but also the retrobulbar fat. GO may occur before, during, or after the onset of hyperthyroidism or, less frequently, in euthyroid or hypothyroid patients.[1] The enlargement of the extraocular muscles is responsible for most of the debilitating manifestations of the disease, including proptosis, diplopia, congestive signs, and DON.[2-5]

DON is a serious complication of GO occurring in 3.4% of patients,[6] almost always as a result of optic nerve compression at the orbital apex by enlarged extraocular muscles. The diagnosis of DON rests mainly on clinical findings such as decreased VA, abnormal VFs, altered color and brightness perception, delayed visual evoked potentials, afferent pupillary defects, and edema or atrophy of the optic nerve head.[7] In many cases, however, DON is subclinical and difficult to diagnose due to confounding signs and symptoms, notably significant orbital congestion or decreased corneal transparency from exposure keratopathy.[8] Establishing a diagnosis of DON may also be difficult because many tests of optic nerve dysfunction, such as VA, color and brightness perception, and VF, especially when performed with standard automated perimetry, require the full cooperation of an alert and motivated patient and will not infrequently render false-positive results, particularly in patients with congestive GO. Because the prognosis of DON improves significantly with early diagnosis and treatment, much effort has been placed on designing objective tests capable of identifying patients at high risk for developing DON.[9]

CT is the preferred imaging technique for investigating DON.[1] Several studies have tested the ability of CT parameters (linear,[3,9-11] area, and volume[12-14] measurements of the orbital muscles) to facilitate the diagnosis of DON. Most of these studies used axial and direct or reformatted coronal images acquired with conventional CT scanners, and calculations were often performed manually from hard copies of the scans. Subjective assessment of apical crowding based on coronal images described by Nugent et al,[15] and detection of intracranial fat prolapse introduced by Birchall et al,[16] have also been used to evaluate the risk of development of DON.

The purpose of this study was to objectively quantify orbital apical crowding by calculating the ratio between extraocular muscle area and orbital bone area at 3 distinct coronal planes using MDCT, and to test the ability of such ratios to detect DON. In addition, we tested for possible correlations

Received October 10, 2011; accepted after revision December 7.

From the Division of Ophthalmology (A.C.P.G., M.L.R.M.) and Department of Radiology (L.N.S., E.M.M.S.G.), University of São Paulo Medical School, São Paulo, Brazil.

Study registered on ClinicalTrial.gov, number NCT00665795.

Please address correspondence to Mário Luiz Ribeiro Monteiro, Av. Angélica 1757 conj 61, 01227-200, São Paulo, Brazil; e-mail: mlrmonteiro@terra.com.br

http://dx.doi.org/10.3174/ajnr.A3029

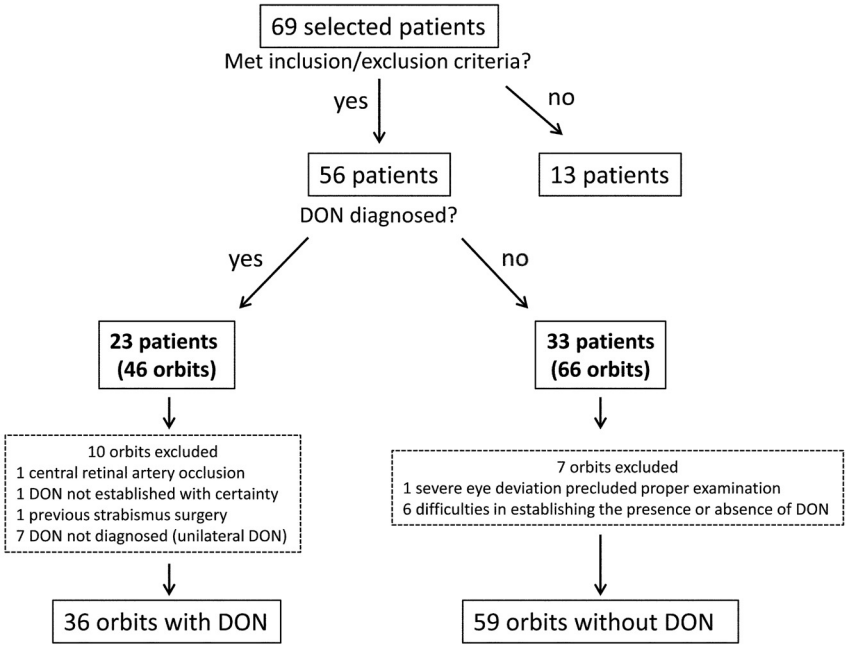

Fig 1. Flow chart demonstrating inclusions and exclusions of patients and orbits, with or without DON, in the study.

between clinical parameters of orbits with DON and CT square area measurements, and we compared the muscle area/bone area ratios calculated with MDCT to assessment of orbital fat prolapse[16] and apical crowding, based on subjective assessment of coronal images.[15]

Materials and Methods

This study followed the principles of the Declaration of Helsinki and was approved by our institutional review board. Sixty-nine patients with GO (47 women, 22 men) were studied prospectively between July 2005 and September 2010. GO was diagnosed in accordance with previously defined criteria.[17] All patients had bilateral GO and symptoms related to the orbitopathy were present for a period of time ranging from 2 weeks to 2 years. Patients underwent a complete neuro-ophthalmologic examination by an experienced neuro-ophthalmologist (M.L.R.M.), including best-corrected VA, applanation tonometry, pupillary reactions, extraocular motility evaluation, slit lamp examination, evaluation of soft tissue and eyelid inflammation, measurement of lid fissure, Hertel exophthalmometry, fundoscopy, and VF evaluation.

VF was performed using manual perimetry and standard automated perimetry. Manual VF testing was performed using the Goldmann perimeter (Haag-Streit, Bern, Switzerland). The V-4-e, I-4-e, I-3-e, I-2-e, and I-1-e stimuli were used to draw the isopters. Kinetic determinations were followed by static presentation of the stimuli, particularly in the central 30-degree area, to search for localized defects. Standard automated perimetry was performed with a Humphrey field analyzer 750 (Zeiss-Humphrey, Dublin, California) using the 24–2 SITA-Standard strategy. The patients' appropriate near correction was used. Rest breaks were allowed when requested. To qualify as an abnormal VF on standard automated perimetry, 3 adjacent abnormal points at $P < .05$, or 2 adjacent points with 1 abnormal point at $P < .01$, were required.[11] Exclusion criteria were age younger than 20 years, poor cooperation for performing VF examination, spherical refraction over ±5 diopters, cylinder correction over ±3 diopters, and an unreliable VF. An unreliable Humphrey VF test was defined as one with greater than 25% fixation losses, false-positive, or false-negative responses. Patients with clinical signs of glaucomatous optic neuropathy, cataract, cornea transparency abnormalities, retinal diseases, previous orbital or strabismus surgery, and other types of neuropathies were also excluded.

Orbits of eyes with GO and visual function data clearly indicating the presence or absence of DON, based on the neuro-ophthalmologic examination, were eligible. The diagnostic criteria for DON were 1) presence of a relative afferent papillary defect, and 2) presence of a well-defined VF defect. Patients with nonreproducible VF abnormalities and ocular or optic nerve diseases preventing correct diagnosis of DON were excluded. All patients with DON had GO in the congestive phase of the disease, with onset of visual disturbance and clinical signs of orbital congestive disease within less than 4 weeks.

Thirteen of the 69 patients did not qualify based on inclusion and exclusion criteria. The remaining 56 patients (36 women) had 95 orbits included in the study, grouped into orbits with and without DON. The first group included 36 orbits of 23 patients with DON. In this group, 10 orbits were not included in the analysis either because DON was unilateral ($n = 7$), the presence or absence of DON could not be established with certainty on 1 side ($n = 2$), or a previous central retinal artery occlusion precluded correct diagnosis of DON ($n = 1$). The second group included 59 orbits from 33 patients in which DON was clearly absent. Seven orbits were excluded from this group because of difficulties in establishing the presence or absence of DON; in 6 cases, VF abnormalities were questionable, even after repeat examination, and in 1 case, severe eye deviation due to extraocular involvement precluded proper VF examination (Fig 1). The data from the 2 groups of orbits were compared.

Within a period of 2 weeks after the clinical examination, all patients were scanned on a 16-section MDCT scanner (MX 8000 IDT16; Philips Medical Systems, Best, the Netherlands) without the use of sedation or intravenous contrast. Patients were scanned with their eyes closed and steady in primary position of gaze. The scanning parameters were 120 Kv, 150 mAs, detector configuration 16 × 0.75 mm, 1.5-mm section thickness, and 0.7-mm section increment. Im-

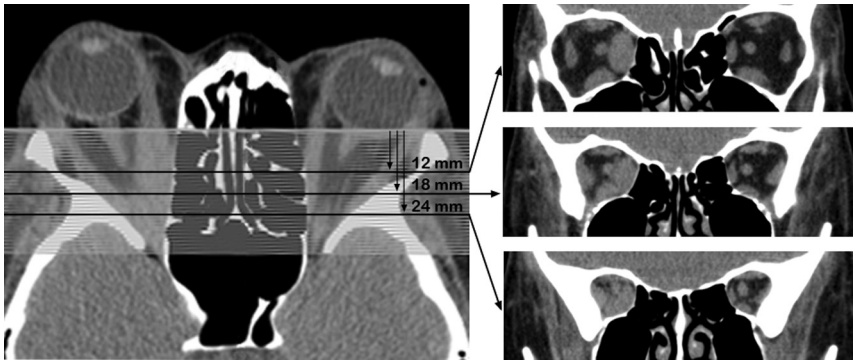

Fig 2. Schematic representation of the CT study. *Left,* Axial scan with planning details of contiguous coronal sections. *Right,* Coronal images taken 12, 18, and 24 mm from the interzygomatic line.

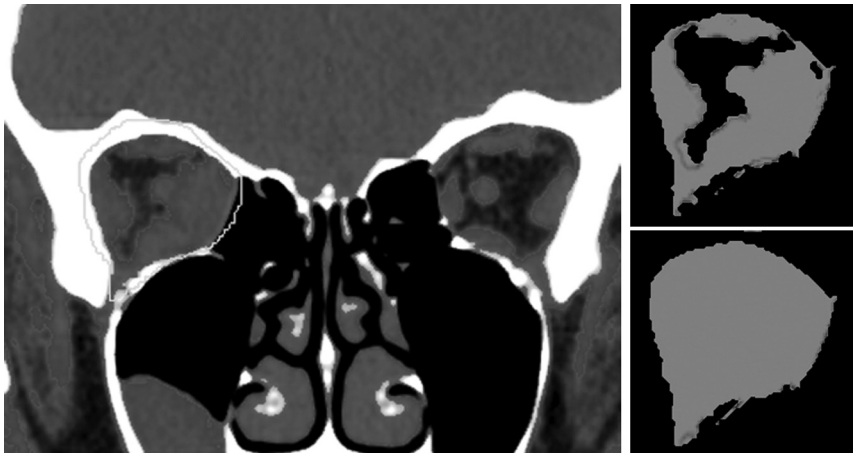

Fig 3. *Left,* Example of reformatted coronal section 18 mm from the interzygomatic line. A region of interest was drawn freehand around the bony orbital rim for automatic calculation of the total area of orbital content (*bottom right).* Area measurements of muscles and soft tissues were obtained based on a predefined range in HU (*top right*). The CI was calculated from the ratio between the soft tissues and the total orbital area. The range of thresholds in HU excluded bone tissue from analysis in all measurements.

ages were postprocessed at a dedicated workstation (Extended Brilliance Workspace V3; Philips Medical Systems) and were analyzed by a head and neck radiologist (L.N.S.) blinded to the clinical condition of the patients.

One-mm coronal slabs were reformatted from contiguous axial sections of the orbit and realigned if any asymmetry was observed. The slabs were reformatted from the orbital rim up to the orbital apex (Fig 2) and evaluated at planes located 12 mm, 18 mm, and 24 mm from that interzygomatic line, defined as the line between the anterior margins of the frontal processes of zygomatic bones at the level of optic nerve plane (Fig 2). Muscular crowding was calculated at each of these planes using a thresholding-based technique (available at the workstation) to calculate the area of extraocular muscle and orbital bone. The software is able to calculate the volumetric measurements of the structures within the slabs. Because we were interested in measuring the area of extraocular muscle and orbital bone, we generated volumes from a 1-mm thick slab, which would correspond numerically to their areas.

A predefined range of threshold was determined to separate soft tissue, which mainly includes muscles, nerves, and vessels from other orbital tissues, which mainly include fat. The thresholds were then set at 40/100 HU (WL/WW) for soft tissue and at −160/230 HU (WL/WW) for the whole orbital content (Fig 3). For each of the preset coronal planes, a region of interest was drawn freehand around the orbital bone rim, so the software could automatically calculate the ratio between the total area of orbital content and the area of soft tissue in the region of interest, thus obtaining the ratio between these as the orbital CI (Fig 3). Bone tissue within the region of interest was not included in any measurement because it is outside the predefined range of thresholds.

The same reader (a practicing radiologist for over 6 years) repeated the measurements for 22 randomly selected orbits (10 with DON) approximately 6 months after the first measurements. On a different occasion, the same group of orbits was independently measured by a senior radiologist (E.M.M.S.G.) with approximately 20 years of practice. Both readers were blinded to the presence or absence of DON.

A categoric score of orbital apical crowding, as described by Nugent et al,[15] was also determined at a predetermined coronal section at the midpoint of the intraorbital optic nerve. The score reflects circumferential effacement of perineural fat by the extraocular muscles (0 = none; 1 = mild, 1%–25%; 2 = moderate, 25%–50%; 3 = severe, >50%).[15] Finally, we assessed each set of images for the presence of intracranial fat prolapse through the superior orbital fissures (recorded as present or absent) using the method described by Birchall et al.[16]

Statistical Analysis

Descriptive statistics included mean values (±SD) for normally distributed variables. Analysis of histograms and the Shapiro-Wilk test were used to evaluate the normality assumption. We used a χ^2 or Fisher exact test for comparison of qualitative variables and an un-

Table 1: Mean ± SD of orbital CI calculated at 12 mm, 18 mm, and 24 mm from the interzygomatic line, and presence or absence of intracranial fat prolapse and categoric scores of orbital crowding (Nugent score) in orbits of patients with GO with or without DON

Parameter	Orbits with DON ($n = 36$)	Orbits without DON ($n = 59$)	*P* value
Mean ± SD 12 mm (95% conf. int)	0.51 ± 0.13 (0.21–0.80)	0.29 ± 0.09 (0.11–0.51)	<0.001*
Mean ± SD 18 mm (95% conf. int)	0.71 ± 0.12 (0.33–0.89)	0.42 ± 0.13 (0.20–0.72)	<0.001*
Mean ± SD 24 mm (95% conf. int)	0.77 ± 0.11 (0.42–1.00)	0.57 ± 0.15 (0.26–0.84)	<0.001*
Intracranial fat prolapse	12 (33.3%)	11 (18.6%)	0.105**
Nugent crowding score ≥1	29 (80.6%)	9 (15%)	<0.001***

Note:—Conf. int. indicates confidence interval.
* Student *t* test.
** χ^2 test.
*** Fisher exact test.

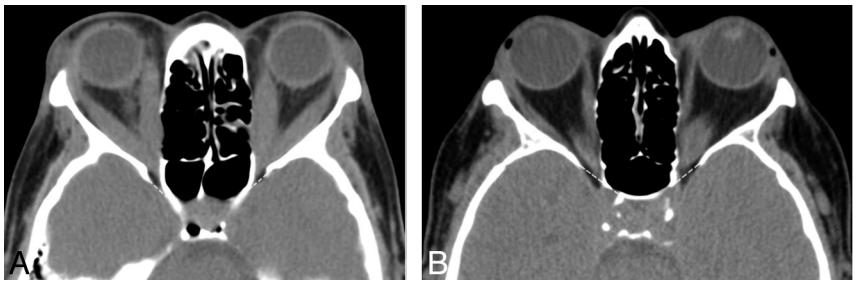

Fig 4. *A,* Axial CT of a patient with bilateral DON and lack of fat prolapse through the superior ophthalmic fissure. The positions of the superior ophthalmic fissures are shown by thin dashed lines. *B,* Axial CT of a patient without DON and showing bilateral fat prolapse through the ophthalmic fissure. The positions of the superior ophthalmic fissures are shown by *thin dashed lines.*

paired *t* test for comparisons of continuous normally distributed parameters corresponding to the mean CIs at planes located 12, 18, and 24 mm from the interzygomatic line. ROC curves were used to describe the ability of CI to discriminate orbits with from those without DON. For each parameter, sensitivities at fixed specificities of 80% and 95% were calculated. ICC was calculated to assess inter- and intrarater variability for measurements of CIs at 12, 18, and 24 mm from the interzygomatic lines. The sensitivity and specificity of the Nugent score and the presence of intracranial prolapse were also calculated. Accuracy and odds ratio for having DON were calculated. Spearman ranked correlation coefficients (ρ) were used to assess the relationship between VF sensitivity loss and the CT parameters analyzed. A *P* value <.05 was considered statistically significant. The statistical analyses were performed using the software SPSS v.15.0 (SPSS, Chicago, Illinois).

Results

Ninety-five orbits of 56 patients with GO met the inclusion criteria and were included in the analysis. Thirty-six of these were from 23 patients (12 women and 11 men; mean age ± SD, 53.6 ± 10.6 years) who met the diagnostic criteria for DON. Fifty-nine orbits were from 33 patients (24 women and 9 men; mean age ± SD, 42.0 ± 10.0 years) affected by GO but not with DON (Fig 1).

The VA of the 36 eyes with DON was 1.0 ($n = 19$), 0.9 ($n = 6$), 0.8 ($n = 5$), 0.6 ($n = 2$), 0.5 ($n = 2$), 0.2 ($n = 1$), and 0.1 ($n = 1$). The mean (± SD) SAP mean deviation in eyes with DON was −10.37 ± 7.38 dB. The glaucoma hemifield test yielded results outside the normal range in 29 eyes and borderline in 5. Exophthalmometry measurements in affected eyes ranged from 19–32 mm (mean ± SD, 25.03 ± 3.11 mm). Restrictive myopathy was present in all orbits with DON. The fundoscopic examination revealed optic disc edema in 6 eyes, optic disc pallor in 1, and no abnormalities in the remainder. In the group without DON, VA was 1.0 in all eyes and exophthalmometry findings ranged from 16.0 to 31.5 mm (mean ± SD, 23.5 ± 2.7).

Table 1 shows mean values (±SD) and range for orbital apex CI values at different positions in the coronal plane, as well as the percentage of orbits with intracranial fat prolapse, in both groups of patients. Table 1 also presents and compares categoric scores of orbital apex crowding (Nugent score) greater than 0 for both groups. In all coronal planes measured, the mean CI values were significantly greater in orbits with DON than in orbits without DON ($P < .001$) There were statistically significant differences between the 2 groups of orbits with regard to the presence of orbital apex crowding, as defined by the Nugent score, but no difference was observed regarding the presence of intracranial fat prolapse (Fig 4).

The ICC for the CI measurements by the second observer at 12, 18, and 24 mm was 0.88, 0.97, and 0.96, respectively ($P < .001$), indicating an excellent interobserver variability. Corresponding values for repeated measurements by the same reader were 0.88, 0.99, and 0.98, indicating excellent intraobserver variability ($P < .001$).

Figure 5 shows ROC curves for the 3 CIs. The area under the ROC curve was 0.91, 0.93, and 0.87 at 12, 18, and 24 mm, respectively, from the interzygomatic plane. In other words, the CI at 18 mm (0.93) was the most efficient indicator of DON. Cutoff values were determined for the 3 indexes to calculate the sensitivity and specificity of the CIs, differentiating the 2 groups of orbits. Sensitivity, specificity, accuracy, and positive and negative predictive values of the categoric scores (Nugent score and intracranial fat prolapse) for the main cutoffs of the 3 CIs are presented in Table 2. The best sensitivity/specificity ratio was found for the CI value of 0.575 at 18 mm from the interzygomatic plane (sensitivity 91.7%, specificity 90.0%, accuracy 90.5, odds ratio for detecting DON 97.2).

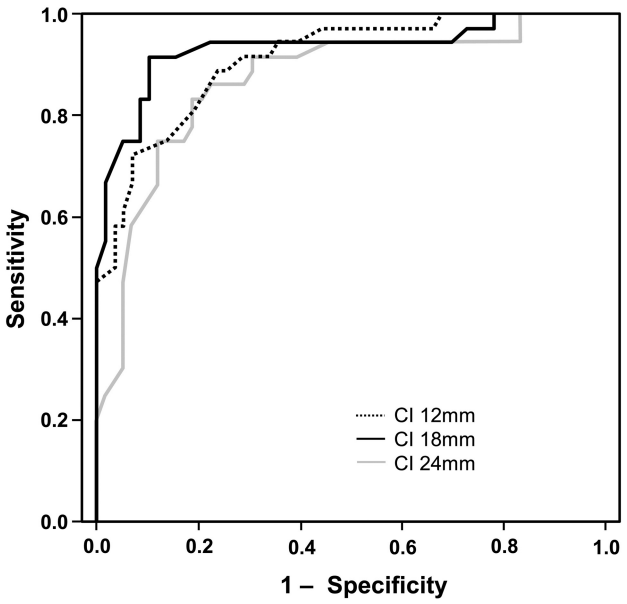

Fig 5. ROC curves of the 3 CI parameters for the discrimination between orbits with and without DON.

Table 3 shows the associations between CT parameters and VF loss based on mean deviation on computerized perimetry. A significant correlation was observed for all parameters studied, but the highest correlation was observed for the parameter CI at 18 mm ($\rho = 0.62$, $R^2 = 38\%$, $P < .001$), with greater CT parameter values associated with greater VF defect (lower mean deviation values). Figure 6 shows a scatterplot of CI measurements at 18 mm from the interzygomatic plane versus VF mean deviation values.

Discussion

A significant complication of GO, DON requires prompt diagnosis and treatment to prevent permanent damage to visual function. Although inflammatory and vascular mechanisms have been suggested, direct compression of the optic nerve by enlarged extraocular muscles at the orbital apex is the most widely accepted theory to explain the development of DON. The theory is based mostly on CT imaging studies confirming the presence of orbital apex crowding in most patients with DON.[10,12,13,18,19]

Because of its great importance in DON, apical crowding is quantified with a score first described by Nugent et al[15] and reproduced by many other authors,[1,3,7,9,16] which grades the effacement of the perineural fat as 0 (none), 1 (up to 25%), 2 (25%–50%), or 3 (greater than 50%).[15] Using this method, Nugent et al found severe apical orbital crowding (grade 3) in 12 of 18 orbits with DON but in only 16 of 124 orbits without DON.[15] Neigel et al graded as moderate or severe crowding 79.2% of orbits with DON but only 12.9% of orbits without DON.[7] Birchall et al found severe apical crowding to be a good predictor of DON, with a sensitivity of 62% and a specificity of 91%.[16] A recent multicenter study found apical muscle crowding in 49 of 56 orbits with DON.[1] In another study, severe optic nerve crowding was retrospectively noted in 80% of orbits (16 of 20) with optic neuropathy compared with 29% of orbits without DON (10 of 34). No orbits with optic neuropathy scored lower than grade 2.[3] Chan et al[9] studied 32 orbits with DON, of which only 2 were given an apical crowding score ≤ 1.

In our study, although the subjective orbital apex CI detected DON with 80.6% sensitivity for scores 1 or 2, none of the 36 affected orbits presented grade 3 apical crowding. These findings are remarkably different from previous studies using the Nugent subjective score to detect DON,[1,3,9,15] probably due to differences in subjective criteria for defining and grading apical crowding. While it seems clear that the Nugent apical crowding score is useful to raise suspicion of the presence of DON, it does not provide a clear definition of the position along the orbit where the coronal plane is used to determine it, nor does it provide a clear differentiation between grades 1, 2, and 3.

We attempted to move 1 step further by objectively quantifying apical crowding at a well-defined coronal plane using MDCT. The technique was made possible by the introduction of MDTC scanners, which make quantitative measures readily available and allow the orbital structures to be reformatted with precision. Our patients were prospectively evaluated for the presence or absence of DON, and a large number of orbits with optic neuropathy were included. Finally, the different CT parameters were submitted to a prospective comparison. Our results show that patients with DON are more efficiently discriminated with the orbital apex crowding score than with the Nugent subjective score, with greater sensitivity/specificity for each index especially at 18 mm from the interzygomatic line. Measurements were found to be reproducible with very high inter- and intraobserver ICC. At all 3 CIs, the 2 groups (with and without DON) differed significantly. The best result was obtained at 18 mm (ROC curve area 0.93). At the 57.5% cutoff, CI at 18 mm reached a sensitivity of 91.7%, a specificity of 89.9% and an odds ratio of 97.2 for detecting DON. This was significantly better than the discrimination ability of both the Nugent score and intracranial fat prolapse (Table 2). It also represents a significant improvement over the performance of the Nugent score in 4 previous studies.[1,3,15,16] Another finding from our study was that, at each point, CI was strongly correlated with VF loss assessed by VF mean deviation (Table 3).

Using MDCT, we revisited the method described by Birchall et al.[16] Unlike the original report, in our study, orbits with or without DON did not differ statistically with regard to intracranial fat prolapse through the superior orbital fissure. MDCT made it possible to view orbital fat prolapse at exactly the same reference points described by the authors, but the results were not predictive of DON in either group. Other researchers have reached similar conclusions.[1,9]

Finally, our study shows that CI is more efficient at detecting DON than the linear muscle index described by Barrett et al.[10] In their study, a muscle index of 67% or greater indicated compressive neuropathy and had a diagnostic sensitivity of 67%.[10] In a previous study using MDCT to determine the sensitivity and specificity of the muscle index in a similar set of patients, we found that a muscle index of 60% provided the best combination of sensitivity/specificity (79% and 72%, respectively).[11]

Other CT features have been studied as indicators of DON, such as lacrimal gland displacement, exophthalmos, superior ophthalmic vein dilation, and single muscle measurements, with poor or inconclusive results.[3,7,10,15,16,19] Chan et al[9] high-

Table 2: Sensitivity, specificity, accuracy, and odds ratio for different cutoff values of CI as well as for Nugent score and the presence of intracranial fat prolapse

Parameter	Cutoff Value	Sensitivity/Specificity	Accuracy (95% conf. int.)	Odds Ratio (95% conf. int.)
Crowding index at 12 mm	38.5%	80.6%/81.4%	80.0 (69.9–87.5)	15.3 (4.9–49.3)
Crowding index at 18 mm	57.5%	91.7%/89.8%	90.5 (0.82–0.95)	97.2 (19.6–572.9)
Crowding index at 24 mm	72.0%	83.3%/81.4%	82.1 (72.3–88.8)	21.8 (6.5–77.2)
Fat prolapse	presence	33.3%/81.4%	0.63 (53.9–72.0)	2.2 (0.8–6.3)
Subjective crowding score	≥1	58.3%/84.7%	74.7 (64.6–82.8)	7.8 (2.7–23.3)

Note:—Conf. int. indicates confidence interval

Table 3: Associations between CT parameters and VF loss expressed in decibels

	VF Loss (dB)	
CT Parameter	ρ*	*P*
Crowding index at 12 mm	0.56	<0.001**
Crowding index at 18 mm	0.62	<0.001**
Crowding index at 24 mm	0.54	<0.001**
Intracranial fat prolapse	0.22	0.033**
Subjective crowding score	0.33	0.001**

*Spearman rank correlation coefficient; ** significant values.

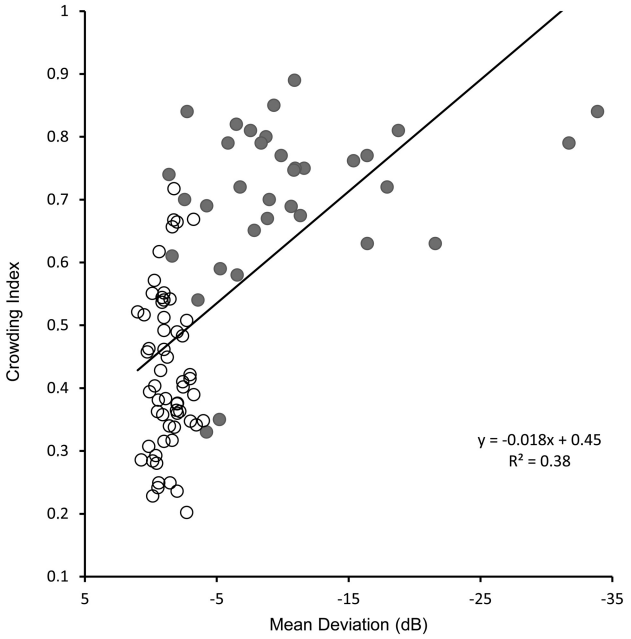

Fig 6. Scatterplots depicting the relationship between CI values measured at 18 mm from the interzygomatic rim and VF mean deviation expressed in decibels in patients with (*closed circles*) or without (*open circles*) DON.

lighted the importance of using both extraocular muscle enlargement and bony orbit anatomy to predict DON, with narrow bony orbits found to be an independent predictor of DON. With our method, because orbital apex CIs express a ratio between the area of soft tissue and the total orbital area, they combine the ability of both parameters to predict DON.

Conclusions

Our study evaluated the ability of the quantitative area index of apical crowding, which is easily calculated on clinical workstations, to predict DON and found it to be an improvement over previously described methods. Further prospective studies will be helpful to validate our findings.

References

1. McKeag D, Lane C, Lazarus JH, et al. **Clinical features of dysthyroid optic neuropathy: a European Group on Graves' Orbitopathy (EUGOGO) survey.** *Br J Ophthalmol* 2007;91:455–58
2. Hallin ES, Feldon SE, Luttrell J. **Graves' ophthalmopathy: III. Effect of transantral orbital decompression on optic neuropathy.** *Br J Ophthalmol* 1988;72:683–87
3. Giaconi JA, Kazim M, Rho T, et al. **CT scan evidence of dysthyroid optic neuropathy.** *Ophthal Plast Reconstr Surg* 2002;18:177–82
4. Monteiro ML, Angotti-Neto H, Benabou JE, et al. **Color Doppler imaging of the superior ophthalmic vein in different clinical forms of Graves' orbitopathy.** *Jpn J Ophthalmol* 2008;52:483–88
5. Monteiro MLR, Moritz RBS, Angotti-Neto H, et al. **Color Doppler imaging of the superior ophthalmic vein in patients with Graves' orbitopathy before and after treatment of congestive disease.** *Clinics (Sao Paulo)* 2011;66:1329–34
6. Ben Simon GJ, Syed HM, Douglas R, et al. **Clinical manifestations and treatment outcome of optic neuropathy in thyroid-related orbitopathy.** *Ophthalmic Surg Lasers Imaging* 2006;37:284–90
7. Neigel JM, Rootman J, Belkin RI, et al. **Dysthyroid optic neuropathy. The crowded orbital apex syndrome.** *Ophthalmology* 1988;95:1515–21
8. Kazim M, Trokel S, Moore S. **Treatment of acute Graves orbitopathy.** *Ophthalmology* 1991;98:1443–48
9. Chan LL, Tan HE, Fook-Chong S, et al. **Graves ophthalmopathy: the bony orbit in optic neuropathy, its apical angular capacity, and impact on prediction of risk.** *AJNR Am J Neuroradiol* 2009;30:597–602
10. Barrett L, Glatt HJ, Burde RM, et al. **Optic nerve dysfunction in thyroid eye disease: CT.** *Radiology* 1988;167:503–07
11. Monteiro ML, Goncalves AC, Silva CT, et al. **Diagnostic ability of Barrett's index to detect dysthyroid optic neuropathy using multidetector computed tomography.** *Clinics (Sao Paulo)* 2008;63:301–06
12. Hallin ES, Feldon SE. **Graves' ophthalmopathy: I. Simple CT estimates of extraocular muscle volume.** *Br J Ophthalmol* 1988;72:674–77
13. Feldon SE, Lee CP, Muramatsu SK, et al. **Quantitative computed tomography of Graves' ophthalmopathy. Extraocular muscle and orbital fat in development of optic neuropathy.** *Arch Ophthalmol* 1985;103:213–15
14. Forbes G, Gorman CA, Brennan MD, et al. **Ophthalmopathy of Graves' disease: computerized volume measurements of the orbital fat and muscle.** *AJNR Am J Neuroradiol* 1986;7:651–56
15. Nugent RA, Belkin RI, Neigel JM, et al. **Graves orbitopathy: correlation of CT and clinical findings.** *Radiology* 1990;177:675–82
16. Birchall D, Goodall KL, Noble JL, et al. **Graves ophthalmopathy: intracranial fat prolapse on CT images as an indicator of optic nerve compression.** *Radiology* 1996;200:123–27
17. Bartley GB, Gorman CA. **Diagnostic criteria for Graves' ophthalmopathy.** *Am J Ophthalmol* 1995;119:792–95
18. Feldon SE, Muramatsu S, Weiner JM. **Clinical classification of Graves' ophthalmopathy. Identification of risk factors for optic neuropathy.** *Arch Ophthalmol* 1984;102:1469–72
19. Kennerdell JS, Rosenbaum AE, El-Hoshy MH. **Apical optic nerve compression of dysthyroid optic neuropathy on computed tomography.** *Arch Ophthalmol* 1981;99:807–09